Optogenetic manipulation of medullary neurons in the locust optic lobe

Hongxia Wang[1], Richard B. Dewell[1], Markus U. Ehrengruber[2], Eran Segev[3], Jacob Reimer[1], Michael L. Roukes[3], Fabrizio Gabbiani[1,4,*]

[1]Department of Neuroscience, Baylor College of Medicine, Houston, TX,
[2]Department of Biology, Kantonsschule Hohe Promenade, Zurich, Switzerland,
[3]Department of Applied Physics and Material Science, California Institute of Technology, Pasadena, CA,
[4]Electrical and Computer Engineering Department, Rice University, Houston, TX

Running Head

Optogenetics in locusts

Address for correspondence

Fabrizio Gabbiani,
Baylor College of Medicine,
Department of Neuroscience,
One Baylor Plaza, Houston, TX, 77030.
Email: gabbiani@bcm.edu
Phone: (713)-798-1849.

Authors' contributions

H.W., M.U.E., J.R., M.L.R. and F.G. designed the experiments; E.S. fabricated the laser probe; H.W. performed the experiments with the assistance of R.B.D and J.R.; H.W. carried out the data analysis with the assistance of R.B.D.; H.W. and F.G. co-wrote the paper.

Abstract

Locust is a widely used animal model for studying sensory processing and its relation to behavior. Due to the lack of genomic information, genetic tools to manipulate neural

circuits in locusts are not yet available. We examined whether Semliki Forest virus is suitable to mediate exogenous gene expression in neurons of the locust optic lobe. We subcloned a channelrhodopsin variant and the yellow fluorescent protein Venus into a Semliki Forest virus vector and injected the virus into the optic lobe of locusts (*Schistocerca americana*). Fluorescence was observed in all injected optic lobes. Most neurons that expressed the recombinant proteins were located in the first two neuropils of the optic lobe, the lamina and medulla. Extracellular recordings demonstrated that laser illumination increased the firing rate of medullary neurons expressing channelrhodopsin. The optogenetic activation of the medullary neurons also triggered firing of a postsynaptic, looming-sensitive neuron, the Lobula Giant Movement Detector (LGMD). These results indicate that Semliki Forest virus is efficient at mediating transient exogenous gene expression and provides a tool to manipulate neural circuits in the locust nervous system and likely other insects.

New and Noteworthy

Using Semliki Forest virus, we efficiently delivered channelrhodopsin into neurons of the locust optic lobe. We demonstrate that laser illumination increases the firing of the medullary neurons expressing channelrhodopsin and of an identified postsynaptic target neuron, the LGMD neuron. This technique allows to manipulate the neuronal activity in locust neural circuits using optogenetics.

Keywords

Locust, optogenetics, medulla, LGMD, Semliki Forest virus

Introduction

Insects are widely used to address fundamental questions about brain mechanisms. Research on insects has broadened our knowledge and helped us understand the neural basis of complex behavior, e.g., communication and navigation in bees and ants (Evangelista et al., 2014; Srinivasan, 2010; Wehner, 2003), vision and motion detection in flies (Egelhaaf, 2008), olfactory learning and odor discrimination in flies, sphinx moths and locusts (Gupta and Stopfer, 2011), auditory processing in crickets (Göpfert and Hennig, 2016), as well as the mechanisms of neural development and genetics, most recently mainly in *Drosophila* (Hales et al., 2015; Spindler and Hartenstein, 2010). In these endeavors, genetic tools are helpful for dissecting neural circuits and deciphering the neural mechanisms underlying different behaviors. The Gal4-UAS system, for instance, is one of the most powerful ways of achieving targeted gene expression in *Drosophila* that has been adapted to other model systems (Asakawa and Kawakami, 2008; Brand and Perrimon, 1993; Busson and Pret, 2007; Imamura et al., 2003). This binary system is widely used to create transgenic flies by combining a driver (Gal4) and responder (UAS) line based on the properties of the yeast transcription factor GAL4 which activates its target genes by binding to UAS *cis*-regulatory sites. Since most neurons in *Drosophila* are small, they are unsuitable for intracellular dendritic recordings, making this model system of limited use for investigations of dendritic computations in single cells. On the other hand, insects with larger neurons such as locusts, crickets or moths have proven optimal for intracellular electrophysiological recordings. In most of these insects, however, it is not easy to manipulate gene expression and carry out genome editing due to lack of genome sequencing information and long generation times. Nevertheless, researchers have developed a variety of genetic tools for several such species. For example, *piggyBac*-derived cassettes have been integrated in the honeybee (*Apis mellifera*) expressing the fluorescent markers Rubia and EGFP under either an artificial or an endogenous promoter (Schulte et al., 2014). In another case, an odorant receptor co-receptor (orco) mutated ant germ line has been generated in *Ooceraea biroi* using CRISPR/Cas gene editing technology (Trible et al., 2017).

Locust is a popular model for studying behavior relying on visual motion, especially

87 visually-evoked escape and collision-avoidance behavior (Fotowat and Gabbiani, 2011).
88 Creating transgenic locust germ lines or developing an efficient neuronal transfection
89 method in locusts would be desirable to increase the power of this model system.
90 However, up to now, there are no known reports on any foreign transformation in the
91 nervous system of locusts. Optogenetics is an efficient stimulation method to control
92 neuronal activity using light-gated ion channels, such as channelrhodopsin,
93 halorhodopsin and their variants (Arrenberg et al., 2009; Boyden et al., 2005; Ishizuka et
94 al., 2006). It has been broadly used to map neural circuitry, study neuronal activity,
95 control cardiac function, and treat photoreceptor degeneration and Parkinson disease
96 (Adamantidis et al., 2007; Arenkiel et al., 2007; Bi et al., 2006; Gradinaru et al., 2009).
97
98 Semliki Forest virus (SFV) is an enveloped single-stranded, positive RNA virus, one of
99 the members in the alphavirus family (Strauss and Strauss, 1994). In earlier work, wild-
100 type SFV and mutant SFV A7(74) were used to drive LacZ and GFP expressions in
101 pyramidal neurons of cultured hippocampal slices (Ehrengruber et al., 1999, 2003).
102 Similarly, the less cytopathic mutant SFV(PD) (Lundstrom et al., 2003) drove protein
103 expression in the rat calyx of Held *in vivo* (Wimmer et al., 2004). Since SFV is a
104 mosquito-borne pathogen, it could possibly infect other non-host insect cells (Lwande et
105 al., 2013), as has been shown for the Sindbis virus (Lewis et al., 1999). To test the
106 possibility that SFV could drive foreign gene expression in locust neurons, we inserted
107 into a SFV A7(74) based vector (Ehrengruber et al., 2003) the channelrhosopin variant,
108 Chop-Wide Receiver (ChopWR), tagged with a fluorescent marker, Venus (Wang et al.,
109 2009) and downstream of a strong ubiquitous promoter. ChopWR is a chimeric protein of
110 Chop1 and Chop2 (Nagel et al., 2003), mediating a larger photocurrent (Wang et al.,
111 2009). This plasmid was electroporated into baby hamster kidney 21 (BHK) cells for
112 generating the virus, which was injected through the eye into the optic lobe of locusts.
113
114 In this paper, we show that viral replicons based on the SFV A7(74) strain successfully
115 express ChopWR-Venus in medullary neurons of the locust optic lobe, enabling us to
116 manipulate optogenetically the activity of medullary neurons and of the LGMD, a
117 downstream neuron which plays a vital role in collision avoidance behavior (Fotowat and

118 Gabbiani, 2011).

119

120 Materials and Methods

121

122 Generation of Semliki Forest virus with ChopWR-Venus and injection in locusts

123 The generation of SFV vectors was described in previous papers (e.g., Ehrengruber et al.,
124 2011). Briefly, the ChopWR-Venus gene was first subcloned into the pENTR2B entry
125 vector and then transferred to the pScaA7-RFA destination vector by using the attB1 and
126 attB2 attachment sites through Gateway Technology (Thermo Fisher Scientific,
127 Waltham, MA). The destination vector pScaA7-RFA was obtained from a modified SFV
128 A7(74) vector plasmid, pSFV(A774nsP) (Ehrengruber et al., 2003), in which the SP6
129 promoter was replaced by CMV/T7 promoters (DiCiommo and Bremner, 1998). The
130 plasmid map of the pScaA7-RFA vector containing ChopWR-Venus is illustrated in Fig.
131 1A. The ChopWR-Venus gene was inserted downstream of the endogenous SFV
132 subgenomic promoter that follows the sequence of SFV non-structural protein 4 (nsP4).
133 Unique restriction sites are indicated in Fig. 1A, as is the simian virus 40 polyadenylation
134 (SV40 polyA) terminator sequence, the Ampicillin resistance gene, and the pBR322
135 origin of replication. The resulting plasmid and the auxiliary plasmid pSFV-helper2 were
136 purified and linearized with the restriction enzyme Spe I (New England Biolabs, Ipswich,
137 MA; NEB). The pENTR2B and pScaA7 plasmids were a gift from Dr. Keith Murai
138 (McGill University) and the pSFV-helper2 plasmid was a gift of Dr. Alan L. Goldin
139 (University of California, Irvine). T7 and Sp6 RNA polymerase (Thermo Fisher
140 Scientific) were used to catalyze the formation of RNAs from linearized pScaA7-
141 ChopWR-Venus and pSFV-helper2 DNAs, respectively. To produce viruses, *in vitro*
142 transcribed RNA from pScaA7-ChopWR-Venus and pSFV-Helper2 were co-
143 electroporated into BHK-21 cells. After that, BHK-21 cells were incubated for 24-48 h in
144 minimum essential (α-MEM) medium containing 5% fetal bovine serum (FBS) at 31 °C
145 with 5% CO_2 (Thermo Fisher Scientific, Waltham, MA). The SFV replicons were
146 harvested and activated by 500 μg/ml α-chymotrypsin for 30 minutes at room
147 temperature, and the reaction was stopped by 250 μg/ml aprotinin (Sigma-Aldrich, St.
148 Louis, MO). The SFV virus titers were $\sim 1 \times 10^5$ infectious particles per ml. Experiments

149 were done using both male and female locusts, *Schistocera americana*, 8-10 weeks old.
150 The locusts were fed with grass sprayed with a solution containing *all-trans*-retinal (1
151 mM, Toronto Research Chemicals, North York, ON, Canada) for 2 days before being
152 injected with ~1-2 μl of viral solution into the right eye using a glass pipette under a
153 Leica stereomicroscope. All protocols were approved by the Bio-Environmental Safety
154 Committee of Baylor College of Medicine.
155
156 **Pilot experiments with other virus expression systems**
157 In preliminary experiments, we tested several additional viral delivery vectors. Sindbis
158 virus with the SP6 promoter was prepared similarly as described above. The titer for
159 Sindbis virus was 5×10^6 infectious particles per ml. Recombinant, GFP-tagged
160 baculovirus with the polyhedrin promoter was purchased from a commercial supplier
161 (#C14, AB Vector; titer: 10^8 pfu/ml). Recombinant adeno-associated virus (AAV)-eGFP
162 with the CMV promoter was a gift from Dr. Matthew Rasband (Baylor College of
163 Medicine; titer: 1×10^{13} GC/ml). In each case, 1-2 μl of solution containing each virus was
164 injected into the locust right eye using a glass pipette under a Leica stereomicroscope.
165 Other procedures were as for the SFV vector.
166
167 **Electrophysiology**
168 The dissection of the locust optic lobe was described in previous papers (e.g., Gabbiani et
169 al., 2002). The LGMD was stained with Alexa 594 by intracellular negative current pulse
170 injection. The Venus-tagged presynaptic neurons, especially their axon terminals, and the
171 LGMD were visualized using two-photon microscopy. The excitation wavelength was set
172 at 830 nm for Alexa 594 and 920 nm for Venus. Sharp electrodes (~10-20 MΩ) were
173 used for intracellular recording from the LGMD. Initially, spikes of the descending
174 contralateral movement detector (DCMD) neuron were recorded extracellularly by
175 positioning hook electrodes around the ventral nerve cord. DCMD spikes allowed us to
176 identify the LGMD in the lobula since they are in one-to-one correspondence with
177 LGMD spikes (O'Shea and Williams, 1974). A 488 nm Cyan Laser (Newport, Model No.
178 PC13589, Ottawa, ON, Canada) with maximum output of 20 mW was used to stimulate
179 ChopWR-expressing neurons in the optic lobe. Medullary neuronal activity was recorded

180 by using a pair of 5 MΩ tungsten electrodes (FHC, Bowdoin, ME; see Wang et al., 2018
181 for details).
182
183 **Optogenetic stimulation**
184 Optic fibers (Thorlabs, Newton, NJ) with diameters of 10, 25 and 200 μm were used to
185 deliver laser light. The optic fiber was connected to the 488 nm Cyan laser via a
186 collimator (F240FC-A, Thorlabs). The area of the incident laser beam arriving at the
187 optic lobe was ~1 mm^2. The laser power was varied between 2 and 20 mW by inserting
188 neutral density filters at the output port of the laser, immediately prior to the collimator,
189 with transmission rates of 10%, 25%, 40%, 63% and 79%, respectively. To restrict the
190 number of activated neurons, a custom-designed laser probe yielding a laser beam with a
191 diameter of ~10 μm was used in a subset of experiments (Segev et al., 2016). The time
192 interval between two successive laser stimulations was 2 minutes to minimize
193 desensitization of the responses. To minimize photoreceptor activation from reflected
194 laser light, the eye was covered with black wax and/or black vinyl tape during laser
195 stimulation. Despite this precaution, light hitting the back of the eye caused small,
196 transient photoreceptor activations when the laser switched on and off.
197
198 **Injection of picrotoxin in the lobula**
199 To investigate whether inhibitory neurons presynaptic to the LGMD had been activated
200 by the laser stimulation, picrotoxin (5 mM; Sigma-Aldrich) dissolved in water was puffed
201 along the dorsal edge of the lobula, close to the region where the inhibitory dendrites of
202 the LGMD's field C arborize. The injected solution contained 0.5 % of the colorant fast
203 green (Sigma-Aldrich) to visualize the tip of the injection pipette and the amount of
204 solution injected in the lobula. The injection pipette's tip diameter varied between 1 and
205 2.5 μm. After injection, the dye diffused around the injection site and stayed confined to
206 the lobula. A picospritzer was used to control the duration and puffing pressure (8 psi/55
207 kPa; WPI, Sarasota, FL). Based on earlier work (Dewell and Gabbiani, 2018), the
208 estimated final concentration of drug at the level of field C was ≤ 200 μM.
209
210 **Data analysis and statistics**

211 Custom Matlab (The MathWorks, Natick, MA) code was used for data analysis. The raw
212 data recorded from medullary neurons were first normalized; the spikes were then
213 detected with a set threshold (see Wang et al., 2018, for details). Spikes within 1.5 ms of
214 a previously detected spike were excluded. To calculate instantaneous firing rates (IFRs)
215 during looming stimuli, the spike train of the LGMD and the medullary neurons were
216 convolved with a Gaussian filter that had a standard deviation of 20 ms. In Fig. 2E, the
217 membrane potential (V_m) of the LGMD was median filtered over a time window of 25 ms
218 to eliminate spikes and reveal the subthreshold V_m time course. For the same reason, in
219 Fig. 2F the average LGMD's V_m during laser stimulation was calculated as its median
220 value during the time interval when the laser was turned on. It was compared with the
221 LGMD's V_m during spontaneous activity, calculated as the median value during the time
222 interval from the start of recording to the start of laser stimulation (>1 s). Medians for
223 each trial where then averaged across 3-5 trials per animal. When using the custom laser
224 probe no spiking was evoked and the LGMD's V_m during laser stimulation was
225 calculated as the mean of V_m during the time when the laser was turned on (Fig. 5B). It
226 was compared with the LGMD's V_m during spontaneous activity, calculated as the mean
227 within 1 s before the start of laser stimulation (Fig. 5C).
228
229 The one-sided Wilcoxon signed-rank test (WSRT) was used to compare the statistical
230 differences between groups of spontaneous activities and activities stimulated by
231 optogenetics with or without picrotoxin treatment. All the data are described as mean ±
232 s.d. (standard deviation).
233
234 **Results**
235
236 **Semliki Forest Virus drives expression of ChopWR-Venus in locust medullary**
237 **neurons**
238 In pilot experiments, we tested with little success the capacity of several viruses to
239 transfect locust optic lobes neurons, including adeno-associated virus (AAV), Sindbis and
240 baculovirus. Although AAV is not known to infect arthropods, other members of its
241 family, as well as Sindbis and baculovirus do (Cotmore et al., 2014; Lewis et al., 1999;

242 Oppenheimer et al., 1999). In contrast, three days after recombinant SFV injection,
243 ChopWR-Venus was observed expressing on the membrane of medullary neurons cell
244 bodies, axonal fibers, and presynaptic terminals in the lobula (Fig. 1B, a-d). When the
245 LGMD was concurrently stained with the fluorescent dye Alexa 594, some axon
246 terminals overlapped with the dendritic branches of the LGMD (Fig. 1B, c, d).
247 Additionally, stained neurons were also observed in the lamina in some experiments,
248 when viral solution was deposited there upon retraction of the injection pipette (not
249 shown). These results indicate that the SFV A7(74) plasmid vector can efficiently deliver
250 a gene of interest into neurons of the medulla (and lamina) of the locust optic lobe. Five
251 of 70 animals injected with virus died; all other locusts were healthy and did not appear
252 to be affected negatively by the manipulation during the experiments.
253
254 **Optogenetic stimulation of medullary neurons activates the LGMD**
255 As demonstrated in Fig. 2A, the instantaneous firing rate (IFR) of transfected medullary
256 neurons increased in response to a 5 s long laser pulse. On average, the spontaneous
257 firing rate of medullary units recorded from a pair of tungsten electrodes was 19.4 ± 12.2
258 spk/s (mean ± s.d.), while optogenetics stimulation increased the rate to 48.9 ± 20.0 spk/s
259 (Fig. 2B). The IFR of the LGMD increased as well (Fig. 2C). On average, the mean firing
260 rate of the LGMD in response to laser stimulation increased from 0 to 7.9 ± 5.1 spk/s
261 (Fig. 2D). The turning ON and OFF of the laser caused brief spike bursts in the medullary
262 neurons (Fig. 2A, arrowheads). Correspondingly, the LGMD fired an initial spike right
263 after the ON transition (Fig. 2C, arrowhead) which was immediately followed by a
264 transient membrane potential (V_m) hyperpolarization of ~1 s duration, also observed right
265 after the laser was turned OFF (Fig. 2E top, arrowheads). During the laser stimulation,
266 the LGMD V_m was depolarized by 3.8 ± 3.0 mV (Fig. 2E, F) in the ChopWR expressing
267 locusts. In uninjected controls, transient responses occurred with laser onset and offset,
268 but no sustained membrane potential depolarization was observed (Fig. 2E bottom).
269 These results imply that optogenetic manipulation of medullary neurons is able to
270 modulate the activity of one downstream target neuron, the LGMD.
271
272 **Block of inhibition enhances LGMD firing to optogenetic stimulation**

273 To isolate the excitatory inputs to the LGMD, the $GABA_A$ receptor antagonist, picrotoxin
274 was puffed at the dorsal edge of the lobula, where inhibitory dendritic branches of the
275 LGMD are located. Compared with the control group, block of inhibition increased the
276 firing of the LGMD in response to the laser stimulation (Fig. 3A and B). The LGMD
277 firing rate caused by the laser stimulation increased from 1.8 ± 0.8 to 7.9 ± 4.3 spk/s after
278 adding picrotoxin (Fig. 3C). Addition of picrotoxin removed the hyperpolarizations
279 observed at the onset and offset of the laser pulse (Fig. 2E), and instead the luminance
280 change caused by the laser turning on and off produced transient bursts with peak firing
281 rates of 69.9 ± 75.1 and 48.8 ± 48.2 spk/s after $GABA_A$ blockade (Fig. 3B, D and E).
282 These results demonstrate that the combination of blocker and optogenetic stimulation
283 was effective at isolating the excitatory input to the LGMD.
284
285 **Laser power affects the firing of the LGMD**
286 Next, we tested whether optogenetic activation of the LGMD depends on the strength of
287 the laser power stimulus used to activate channelrhodopsin. As demonstrated for one
288 example in Fig. 4A, the mean number of spikes of the LGMD across 5 trials increased
289 from 19.8 ± 3.3 to 44.6 ± 14.7 when power increased from 2 to 8 mW. However, at the
290 higher power of 16 mW, the number of LGMD spikes elicited by the laser stimulus was
291 slightly lower, 33.2 ± 11.9. We further investigated the effect of laser power in 5 animals
292 by using 6 values varying from 2 to 20 mW (Fig. 4B). As shown in Fig. 4B, we found
293 that spiking increased when power was increased from 2 to 5 and 8 mW (18.4 ± 6.2, 31.3
294 ± 19.1 and 37.7 ± 23.3, respectively). However, higher powers of 13, 16 and 20 mW
295 resulted in slightly decreased spiking output than at 8 mW (28.2 ± 19.0, 28.4 ± 16.9 and
296 30.6 ± 17.4, respectively). The decrement might be caused by desensitization of channel
297 rhodopsin at stronger laser power (Lin, 2011; Wang et al., 2009). These results indicate
298 that optogenetic activation of the LGMD can be modulated by the laser power strength
299 for a given expression level of Chop-WR in medullary neurons.
300
301 **Narrow laser beam produces less LGMD activation**
302 When we varied the diameter of the optic fibers used to deliver the stimulus to the optic
303 lobe from 10 to 200 μm we found that the illuminated region did not change much,

always being ~1 mm^2. To further spatially restrict the number of neurons activated by the laser stimulus, we replaced the optic fiber with a specialized custom laser probe with an exit beam diameter of 10 μm (Fig. 5A; Methods). As demonstrated in Fig. 5B, illumination transmitted by this laser probe triggered EPSPs but no spiking in the LGMD, except for the spikes evoked by the on and off stimulation caused by the laser light onset and offset. The average LGMD's V_m during laser probe illumination was significantly depolarized 0.5 ± 0.3 mV and 0.2 ± 0.3 mV in the first 2 s and over the whole duration of laser illumination. These results indicate that the modified laser probe is suitable for restricting the number of neurons activated by laser light.

Discussion

In this study, we demonstrated that SFV A7(74) drove ChopWR-Venus expression on the cell membrane of medullary neurons in the locust optic lobe. Laser illumination increased the firing rate of the medullary neurons expressing ChopWR-Venus and triggered the firing of a downstream lobula neuron, the LGMD, which plays a key role in the locust visual collision-detection circuit. SFV A7(74) mediated highly efficient expression of ChopWR-Venus and led to the labelling of many neurons in the region surrounding the injection site. These findings provide a way to express genes of interest in locust neurons and to modulate neuronal activity using optogenetics. Besides optogenetics, GCaMP calcium indicators (Akerboom et al., 2012) are future candidates for expression in locust medullary neurons via SFV A7(74) transfection. These tools will help identify anatomically medullary neurons and study their roles in specific visual processing tasks through characterization of their calcium responses to different visual stimuli.

The responses immediately after the laser onset and offsets (arrowheads in Fig. 2; initial spikes in Figs. 3 and 4) were likely caused, in part, by photoreceptor activation from scattered laser light hitting the back of the eye. In experiments without viral transfection, no prolonged change in LGMD activity occurred in response to laser stimulation (Fig. 2E, bottom). The prolonged activation of medullary neurons and the LGMD during laser illumination were not attributable to the activation of photoreceptors, and therefore are

335 believed to be solely due to the light-gated ChopWR current influx into the medullary
336 neurons.
337
338 Because the large number of medullary neurons expressing ChopWR-Venus contained a
339 mixture of both excitatory and inhibitory neurons, it was hard to precisely control
340 neuronal activation of the LGMD through optogenetic stimulation. Reducing the area of
341 laser illumination is one way to get more specific activation. We tested a specialized
342 custom laser probe that minimizes the size of the laser beam and thus limits the number
343 neurons activated (Fig. 5). In this configuration, only EPSPs but no spikes were evoked
344 in the LGMD by optogenetic stimulation. However, a cell-type specific pattern of neural
345 activation could not be achieved with currently available tools. In genetic model systems
346 such as mice and fruit flies there are ways to generate cell-type specific gene expression.
347 In mice, for example, the Cre-LoxP system drives cell-type specific expression through
348 defined promoters (Sauer, 1998). In flies, the Gal4-UAS binary system mentioned above
349 achieves the same goal (Busson and Pret, 2007). For transient gene expression in locusts,
350 it would also be desirable to target genes to specific cell types. However, this is not yet
351 feasible due to lack of identification of cell-type specific promoters and of transgenic
352 locust lines expressing an effector gene under their control.
353
354 Yet, other possibilities to target gene expression in specific cell types exist. Micro RNAs
355 (miRNAs) are small noncoding RNAs involved in posttranscriptional regulation of gene
356 expression (Obernosterer et al., 2006). Recently, miRNAs have been applied to de-target
357 gene expression when using a SFV-derived oncolytic virus to treat tumors such as
358 glioblastoma (Ramachandran et al., 2017; Ylösmäki et al., 2013). The working principle
359 of miRNAs is that by integrating the complementary sequence of a miRNA in the viral
360 genome downstream of the viral subgenomic promoter, the miRNAs expressed in
361 specific cells can identify the complementary sequence and cause the degradation of viral
362 mRNA. This in turn reduces the expression of viral proteins in those cells. Wild-type
363 SFV is naturally neurotropic (e.g., Ehrengruber et al., 1999). So, to protect neurons from
364 SFV based cancer virotherapy, the neuron-specific miRNAs, miR124, miR125, and
365 miR134 were inserted into the SFV4 vector genome. This resulted in attenuated neuro-

366 virulence in cultured neurons, astrocytes, and oligodendrocytes, and it also attenuated
367 neurovirulence in adult mice, but the modified virus retained its replication ability in
368 murine neural stem cells where the expression of these miRNAs is low (Ramachandran et
369 al., 2017; Ylösmäki et al., 2013).
370
371 Interestingly, abundant miRNAs have been identified in tissues of a species closely
372 related to that studied here, *Locusta migratoria*, including the pronotum, testes, antennae,
373 fat bodies, and brains (Wang et al., 2015). Homology searches indicated that tissue-
374 specific miRNAs were also lineage-specific and that many of them were specifically
375 expressed in the brain. Thus, provided information becomes available in the future on the
376 expression pattern of the miRNAs in specific cell populations, such as excitatory or
377 inhibitory neurons, one could add their complementary sequence to SFV plasmids and
378 obtain specific gene expression in the locust.
379
380 Injecting a viral vector containing a gene of interest in insects will only produce transient
381 expression. Creating a transgenic line would be optimal to get stable foreign gene
382 expression. Although there are no reported transgenic locusts, transgenic houseflies
383 (Hediger et al., 2001), silkworms (Tamura et al., 2000), ants (Trible et al., 2017),
384 honeybees (Schulte et al., 2014), and crickets (Nakamura et al., 2010) have been created
385 using a transposon *piggyBac*-derived vector. In the locust, one recently identified miRNA
386 precursor is likely a transposable element (TE) from a long-interspersed element family
387 (Wang et al., 2015). One could thus try this putative locust specific transposable element
388 or use the transposon *piggyBac*-derived vector described by Nakamura et al. (2010) to
389 generate germ transformation.
390
391 **Acknowledgements**
392 We thank Dr. Hiromu Yawo and Dr. Toru Ishizuka for providing pChopWR-Venus. We
393 also thank Dr. Emma Victoria Jones and Dr. Keith Murai for providing the plasmids
394 pENTR2B and pScaA7-RFA, and Dr. Alan L. Goldin for pSFV-Helper2.
395
396 **Grants**

397 This work was supported by a grant from the NIH (MH-065339) and the NSF (IIS-
398 1607518).

399

400 **Disclosures**

401 The authors declare no competing financial interests.

402

403 ## References

404 Adamantidis, A.R., Zhang, F., Aravanis, A.M., Deisseroth, K., and de Lecea, L. (2007).
405 Neural substrates of awakening probed with optogenetic control of hypocretin
406 neurons. Nature *450*, 420–424.

407 Akerboom, J., Chen, T.-W., Wardill, T.J., Tian, L., Marvin, J.S., Mutlu, S., Calderon, N.C.,
408 Esposti, F., Borghuis, B.G., Sun, X.R., et al. (2012). Optimization of a GCaMP Calcium
409 Indicator for Neural Activity Imaging. Journal of Neuroscience *32*, 13819–13840.

410 Arenkiel, B.R., Peca, J., Davison, I.G., Feliciano, C., Deisseroth, K., Augustine, G.J.,
411 Ehlers, M.D., and Feng, G. (2007). In Vivo Light-Induced Activation of Neural
412 Circuitry in Transgenic Mice Expressing Channelrhodopsin-2. Neuron *54*, 205–218.

413 Arrenberg, A.B., Del Bene, F., and Baier, H. (2009). Optical control of zebrafish
414 behavior with halorhodopsin. Proceedings of the National Academy of Sciences *106*,
415 17968–17973.

416 Asakawa, K., and Kawakami, K. (2008). Targeted gene expression by the Gal4-UAS
417 system in zebrafish. Development, Growth & Differentiation *50*, 391–399.

418 Bi, A., Cui, J., Ma, Y.-P., Olshevskaya, E., Pu, M., Dizhoor, A.M., and Pan, Z.-H. (2006).
419 Ectopic Expression of a Microbial-Type Rhodopsin Restores Visual Responses in
420 Mice with Photoreceptor Degeneration. Neuron *50*, 23–33.

421 Boyden, E.S., Zhang, F., Bamberg, E., Nagel, G., and Deisseroth, K. (2005). Millisecond-
422 timescale, genetically targeted optical control of neural activity. Nature
423 Neuroscience *8*, 1263–1268.

424 Brand, A.H., and Perrimon, N. (1993). Targeted gene expression as a means of
425 altering cell fates and generating dominant phenotypes. Development *118*, 401–415.

426 Busson, D., and Pret, A.-M. (2007). GAL4/UAS Targeted Gene Expression for
427 Studying Drosophila Hedgehog Signaling. In Hedgehog Signaling Protocols, (Totowa,
428 NJ: Humana Press), pp. 161–201.

429 Cotmore, S.F., Agbandje-McKenna, M., Chiorini, J.A., Mukha, D.V., Pintel, D.J., Qiu, J.,
430 Soderlund-Venermo, M., Tattersall, P., Tijssen, P., Gatherer, D., et al. (2014). The

431 family <Emphasis Type="Italic">Parvoviridae</Emphasis>. Arch Virol *159*, 1239–
432 1247.

433 Dewell, R.B., and Gabbiani, F. (2018). Biophysics of object segmentation in a
434 collision-detecting neuron. ELife *7*, e34238.

435 DiCiommo, D.P., and Bremner, R. (1998). Rapid, High Level Protein Production Using
436 DNA-based Semliki Forest Virus Vectors. Journal of Biological Chemistry *273*,
437 18060–18066.

438 Egelhaaf, M. (2008). Fly vision: neural mechanisms of motion computation. Curr.
439 Biol. *18*, R339-341.

440 Ehrengruber, M.U., Lundstrom, K., Schweitzer, C., Heuss, C., Schlesinger, S., and
441 Gähwiler, B.H. (1999). Recombinant Semliki Forest virus and Sindbis virus
442 efficiently infect neurons in hippocampal slice cultures. Proc. Natl. Acad. Sci. U.S.A.
443 *96*, 7041–7046.

444 Ehrengruber, M.U., Renggli, M., Raineteau, O., Hennou, S., Vähä-Koskela, M.J.V.,
445 Hinkkanen, A.E., and Lundstrom, K. (2003). Semliki Forest virus A7(74) transduces
446 hippocampal neurons and glial cells in a temperature-dependent dual manner. J.
447 Neurovirol. *9*, 16–28.

448 Ehrengruber, M.U., Schlesinger, S., and Lundstrom, K. (2011). Alphaviruses: Semliki
449 Forest Virus and Sindbis Virus Vectors for Gene Transfer into Neurons. Current
450 Protocols in Neuroscience *57*, 4.22.1-4.22.27.

451 Evangelista, C., Kraft, P., Dacke, M., Labhart, T., and Srinivasan, M.V. (2014).
452 Honeybee navigation: critically examining the role of the polarization compass.
453 Philos. Trans. R. Soc. Lond., B, Biol. Sci. *369*, 20130037.

454 Fotowat, H., and Gabbiani, F. (2011). Collision Detection as a Model for Sensory-
455 Motor Integration. Annual Review of Neuroscience *34*, 1–19.

456 Gabbiani, F., Krapp, H.G., Koch, C., and Laurent, G. (2002). Multiplicative computation
457 in a visual neuron sensitive to looming. Nature *420*, 320–324.

458 Göpfert, M.C., and Hennig, R.M. (2016). Hearing in Insects. Annual Review of
459 Entomology *61*, 257–276.

460 Gradinaru, V., Mogri, M., Thompson, K.R., Henderson, J.M., and Deisseroth, K. (2009).
461 Optical Deconstruction of Parkinsonian Neural Circuitry. Science *324*, 354–359.

462 Gupta, N., and Stopfer, M. (2011). Insect olfactory coding and memory at multiple
463 timescales. Current Opinion in Neurobiology *21*, 768–773.

464 Hales, K.G., Korey, C.A., Larracuente, A.M., and Roberts, D.M. (2015). Genetics on the
465 Fly: A Primer on the Drosophila Model System. Genetics *201*, 815–842.

466 Hediger, M., Niessen, M., Wimmer, E.A., Dübendorfer, A., and Bopp, D. (2001).
467 Genetic transformation of the housefly Musca domestica with the lepidopteran
468 derived transposon piggyBac: Genetic transformation in Musca. Insect Molecular
469 Biology *10*, 113–119.

470 Imamura, M., Nakai, J., Inoue, S., Quan, G.X., Kanda, T., and Tamura, T. (2003).
471 Targeted Gene Expression Using the GAL4/UAS System in the Silkworm Bombyx
472 mori. Genetics *165*, 1329–1340.

473 Ishizuka, T., Kakuda, M., Araki, R., and Yawo, H. (2006). Kinetic evaluation of
474 photosensitivity in genetically engineered neurons expressing green algae light-
475 gated channels. Neuroscience Research *54*, 85–94.

476 Lewis, D.L., DeCamillis, M.A., Brunetti, C.R., Halder, G., Kassner, V.A., Selegue, J.E.,
477 Higgs, S., and Carroll, S.B. (1999). Ectopic gene expression and homeotic
478 transformations in arthropods using recombinant Sindbis viruses. Curr. Biol. *9*,
479 1279–1287.

480 Lin, J.Y. (2011). A User's Guide to Channelrhodopsin Variants: Features, Limitations
481 and Future Developments. Exp Physiol *96*, 19–25.

482 Lundstrom, K., Abenavoli, A., Malgaroli, A., and Ehrengruber, M.U. (2003). Novel
483 semliki forest virus vectors with reduced cytotoxicity and temperature sensitivity
484 for long-term enhancement of transgene expression. Molecular Therapy *7*, 202–209.

485 Lwande, O.W., Lutomiah, J., Obanda, V., Gakuya, F., Mutisya, J., Mulwa, F., Michuki, G.,
486 Chepkorir, E., Fischer, A., Venter, M., et al. (2013). Isolation of Tick and Mosquito-
487 Borne Arboviruses from Ticks Sampled from Livestock and Wild Animal Hosts in
488 Ijara District, Kenya. Vector-Borne and Zoonotic Diseases *13*, 637–642.

489 Nagel, G., Szellas, T., Huhn, W., Kateriya, S., Adeishvili, N., Berthold, P., Ollig, D.,
490 Hegemann, P., and Bamberg, E. (2003). Channelrhodopsin-2, a directly light-gated
491 cation-selective membrane channel. Proceedings of the National Academy of
492 Sciences *100*, 13940–13945.

493 Nakamura, T., Yoshizaki, M., Ogawa, S., Okamoto, H., Shinmyo, Y., Bando, T., Ohuchi,
494 H., Noji, S., and Mito, T. (2010). Imaging of Transgenic Cricket Embryos Reveals Cell
495 Movements Consistent with a Syncytial Patterning Mechanism. Current Biology *20*,
496 1641–1647.

497 Obernosterer, G., Leuschner, P.J.F., Alenius, M., and Martinez, J. (2006). Post-
498 transcriptional regulation of microRNA expression. RNA *12*, 1161–1167.

499 Oppenheimer, D.I., MacNicol, A.M., and Patel, N.H. (1999). Functional conservation of
500 the wingless-engrailed interaction as shown by a widely applicable baculovirus
501 misexpression system. Curr. Biol. *9*, 1288–1296.

502 O'Shea, M., and Williams, J.L.D. (1974). The anatomy and output connection of a
503 locust visual interneurone; the lobular giant movement detector (LGMD) neurone.
504 Journal of Comparative Physiology A: Neuroethology, Sensory, Neural, and
505 Behavioral Physiology *91*, 257–266.

506 Ramachandran, M., Yu, D., Dyczynski, M., Baskaran, S., Zhang, L., Lulla, A., Lulla, V.,
507 Saul, S., Nelander, S., Dimberg, A., et al. (2017). Safe and Effective Treatment of
508 Experimental Neuroblastoma and Glioblastoma Using Systemically Delivered Triple
509 MicroRNA-Detargeted Oncolytic Semliki Forest Virus. Clinical Cancer Research *23*,
510 1519–1530.

511 Sauer, B. (1998). Inducible Gene Targeting in Mice Using the Cre/loxSystem.
512 Methods *14*, 381–392.

513 Schulte, C., Theilenberg, E., Müller-Borg, M., Gempe, T., and Beye, M. (2014). Highly
514 efficient integration and expression of piggyBac-derived cassettes in the honeybee
515 (Apis mellifera). Proc. Natl. Acad. Sci. U.S.A. *111*, 9003–9008.

516 Segev, E., Reimer, J., Moreaux, L.C., Fowler, T.M., Chi, D., Sacher, W.D., Lo, M.,
517 Deisseroth, K., Tolias, A.S., Faraon, A., et al. (2016). Patterned photostimulation via
518 visible-wavelength photonic probes for deep brain optogenetics. Neurophotonics *4*,
519 011002.

520 Spindler, S.R., and Hartenstein, V. (2010). The Drosophila neural lineages: a model
521 system to study brain development and circuitry. Dev. Genes Evol. *220*, 1–10.

522 Srinivasan, M.V. (2010). Honey bees as a model for vision, perception, and cognition.
523 Annu. Rev. Entomol. *55*, 267–284.

524 Strauss, J.H., and Strauss, E.G. (1994). The alphaviruses: gene expression, replication,
525 and evolution. Microbiol. Rev. *58*, 491–562.

526 Tamura, T., Thibert, C., Royer, C., Kanda, T., Eappen, A., Kamba, M., Kômoto, N.,
527 Thomas, J.-L., Mauchamp, B., Chavancy, G., et al. (2000). Germline transformation of
528 the silkworm Bombyx mori L. using a piggyBac transposon-derived vector. Nature
529 Biotechnology *18*, 81–84.

530 Trible, W., Olivos-Cisneros, L., McKenzie, S.K., Saragosti, J., Chang, N.-C., Matthews,
531 B.J., Oxley, P.R., and Kronauer, D.J.C. (2017). orco Mutagenesis Causes Loss of
532 Antennal Lobe Glomeruli and Impaired Social Behavior in Ants. Cell *170*, 727-
533 735.e10.

534 Wang, H., Sugiyama, Y., Hikima, T., Sugano, E., Tomita, H., Takahashi, T., Ishizuka, T.,
535 and Yawo, H. (2009). Molecular determinants differentiating photocurrent
536 properties of two channelrhodopsins from chlamydomonas. J. Biol. Chem. *284*,
537 5685–5696.

538 Wang, Y., Jiang, F., Wang, H., Song, T., Wei, Y., Yang, M., Zhang, J., and Kang, L. (2015).
539 Evidence for the expression of abundant microRNAs in the locust genome. Scientific
540 Reports *5*, 13608.

541 Wehner, R. (2003). Desert ant navigation: how miniature brains solve complex
542 tasks. J Comp Physiol A *189*, 579–588.

543 Wimmer, V.C., Nevian, T., and Kuner, T. (2004). Targeted in vivo expression of
544 proteins in the calyx of Held. Pflugers Arch - Eur J Physiol *449*, 319–333.

545 Ylösmäki, E., Martikainen, M., Hinkkanen, A., and Saksela, K. (2013). Attenuation of
546 Semliki Forest Virus Neurovirulence by MicroRNA-Mediated Detargeting. J. Virol. *87*,
547 335–344.

548

549

550 **Figure Legends**

551

552 **Figure 1.** Semliki Forest Virus (SFV) drives Chop-wide receiver (ChopWR)-Venus
553 expression in medullary neurons of the locust optic lobe. **A**, Schematic diagram showing
554 the plasmid used to generate the SFV A7(74) based vectors encoding ChopWR-Venus.
555 The viral backbone is derived from pSFV(A774nsP) (Ehrengruber, et al. 2003). **B**, a),
556 Medullary neurons somata expressed ChopWR-Venus in the locust optic lobe (white
557 arrows). b), Bundles of transmedullary axons expressing ChopWR-Venus (white arrow)
558 travel towards the lobula neuropil (grey arrow). c) and d), Double stain of the LGMD
559 excitatory dendritic field (Alexa 594, red) and Venus-labeled transmedullary neuron
560 terminal arbors (green) show close apposition in the lobula. Abbreviations, *L*: lateral, *M*:
561 medial, *D*: dorsal, *V*: ventral. Scale bars are listed in each panel.

562

563 **Figure 2.** Laser stimulation via optic fiber with a diameter of 200 μm activated the
564 medullary neurons (Med) expressing ChopWR-Venus and the LGMD. **A,** The
565 instantaneous firing rate of the medullary neurons expressing ChopWR-Venus was
566 increased during 5 s of 488 nm laser stimulation; top, laser stimulation timing; bottom,
567 blue trace is the averaged firing rate across 4 trials (light blue traces). Rasters below the
568 IFR show the medullary neuronal spikes. **B**, The mean firing rate of the medullary
569 neurons expressing ChopWR-Venus across 6 locusts (red dots) was compared with and
570 without laser stimulation; * indicates p = 0.0156 (one-sided WSRT). **C,** The
571 instantaneous firing rate of the LGMD increased during 5 s of 488 nm laser stimulation;
572 green trace is the averaged firing rate across 4 trials (light green traces). Rasters below
573 the IFR show the LGMD spikes. **D**, The mean firing rate of the LGMD across 6 locusts
574 (red dots) was compared with and without laser stimulation; * indicates p = 0.0156. **E**,

575 The LGMD V_m was depolarized during 5 s of 488 nm laser stimulation in a ChopWR-
576 expressing locust (top), while no depolarization was observed in an un-transfected control
577 (bottom). Black trace represents the averaged V_m and gray traces are individual trials (4
578 trials in the ChopWR-expressing locust and 6 trials in the wild type locust). **F**, Plot of the
579 mean median LGMD V_m (± 1 s.d.) with and without laser stimulation in 6 animals. *
580 indicates p = 0.0156.
581
582 **Figure 3.** Laser stimulation triggers inhibitory inputs to the LGMD that can be blocked
583 by the $GABA_A$ receptor antagonist picrotoxin (PTX). **A**, Laser stimulation (2 s, 488 nm)
584 via an optic fiber with diameter of 10 μm triggered the firing of the LGMD. Top, laser
585 stimulation timing; middle, the LGMD V_m from 1 trial; bottom, the averaged LGMD IFR
586 (gray trace) across 5 trials (light gray traces). The rasters below are the spikes of the
587 LGMD from 5 trials. **B**, Puffing PTX increased laser-triggered firing in the LGMD. Top,
588 laser stimulation timing; middle, the LGMD V_m from 1 trial; bottom, the averaged
589 LGMD IFR (gray trace) across 5 trials (light gray traces). The rasters below are the
590 spikes of the LGMD from 5 trials. **C**, The mean firing rate of the LGMD triggered by
591 laser stimulation was compared with and without puffing PTX. **D** and **E**, mean firing rate
592 of the LGMD triggered by laser onset (D) and offset (E) were compared with and without
593 puffing PTX. Red symbols indicated the mean values across 3 locusts.
594
595 **Figure 4**. The firing of the LGMD increased and saturated in response to increasing laser
596 power. **A**, Examples of the LGMD IFR in response to laser powers of 2, 8 and 16 mW
597 (from top to bottom; one locust). Laser stimulation timing is shown above the top panel
598 (duration: 5 s). Each panel shows the averaged LGMD IFR (dark purple) from 5 trials
599 (light purple). The rasters below the LGMD IFR are the LGMD spikes from the 5 trials
600 (p = 0.0312 and 0.125 between groups with laser power at 2 vs. 8 and 8 vs. 16 mW by a
601 one-sided WSRT). **B**, The number of LGMD spike evoked by laser stimulation increased
602 and saturated with increasing power. Blue circles indicate the mean value in each group.
603 A Kruskal-Wallis test was used to evaluate the effect of laser power across groups
604 (p=0.013). A post-hoc signed rank test was used to evaluate the difference between two
605 groups (p values on panel; ns, no significant difference).
606
607 **Figure 5.** A laser probe narrowing the region activated by the laser elicited only EPSPs in
608 the LGMD. **A**, Schematics of the laser probe (left) and optic fiber (right). Dashed lines
609 indicate light path. In the laser probe, the beam exits perpendicular to the shaft thanks to a
610 mirror. **B**, Laser probe stimulation (5 s, 488 nm) triggered EPSPs in the LGMD. Top,
611 laser stimulation timing; bottom, the averaged LGMD V_m (black trace) across 4 trials
612 (gray traces). **C**, Comparison of the mean across 3-5 trials of the LGMD V_m (± 1 s.d.) for
613 5 locusts with and without laser stimulation. For each animal the mean V_m was higher
614 during the laser stimulation and higher during the first 2 s than the last 3 s of laser
615 stimulation. * indicates p = 0.0312 by a one-sided WSRT.
616

A

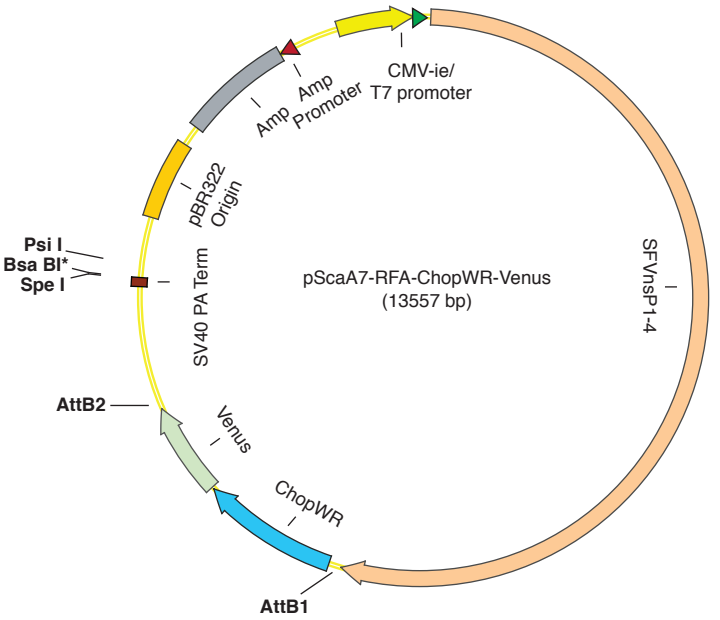

B

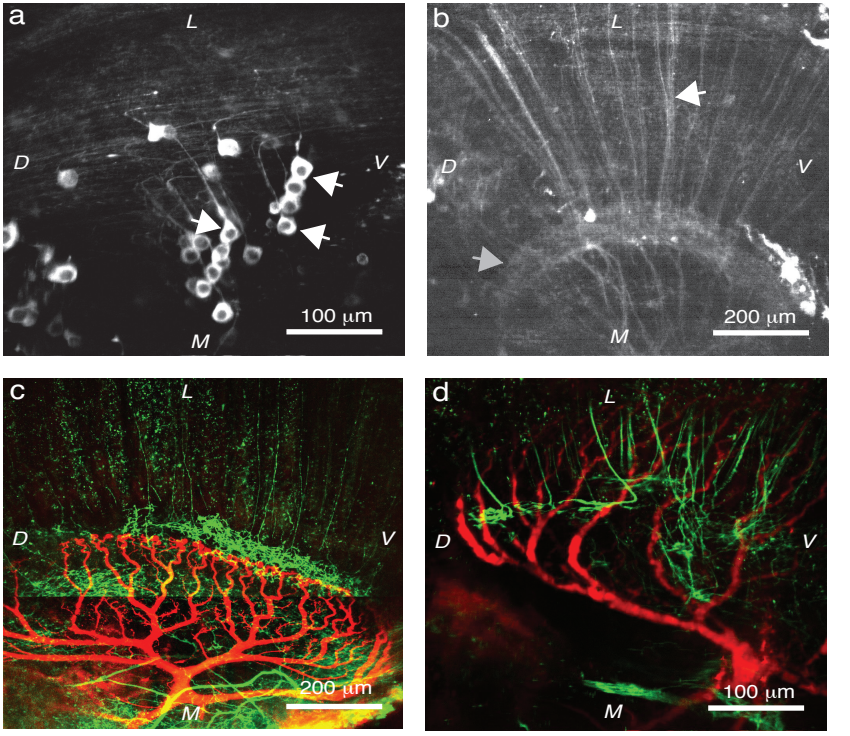

Wang et al., Fig. 1

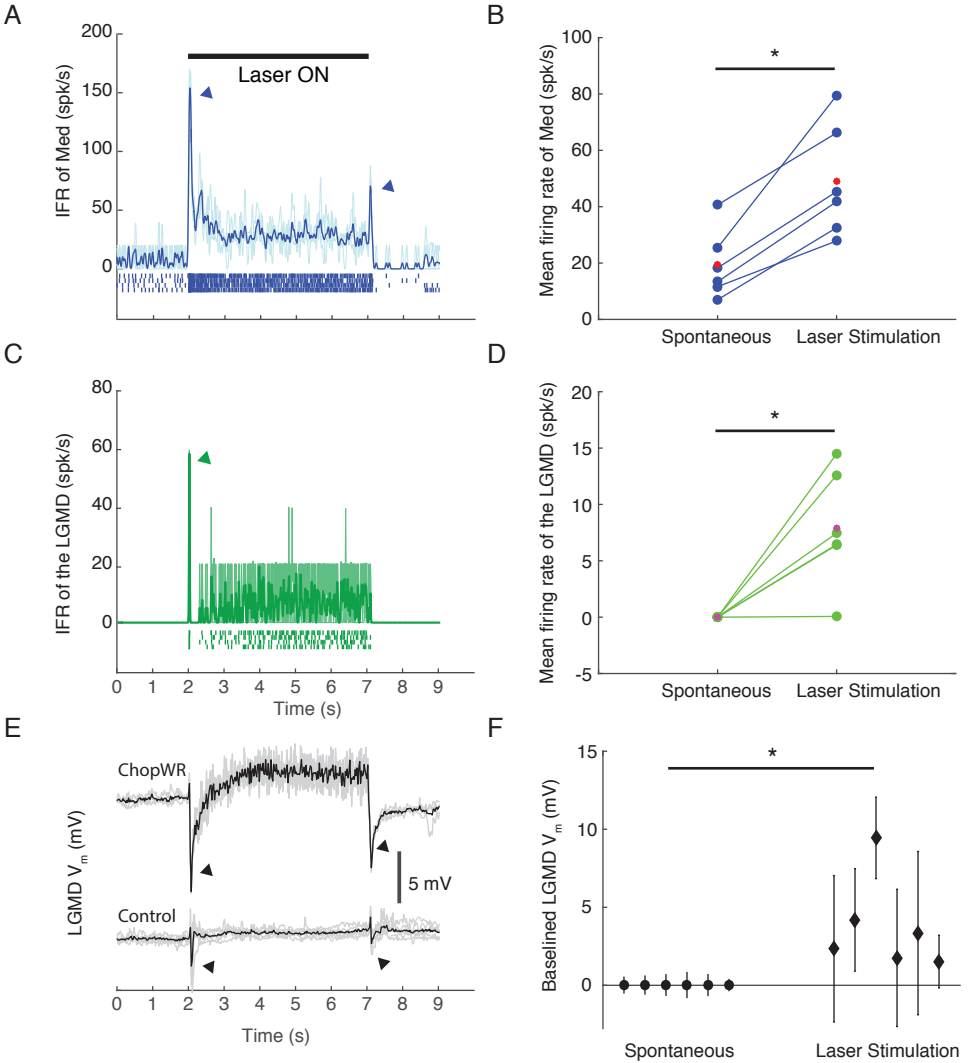

Wang et al., Fig. 2

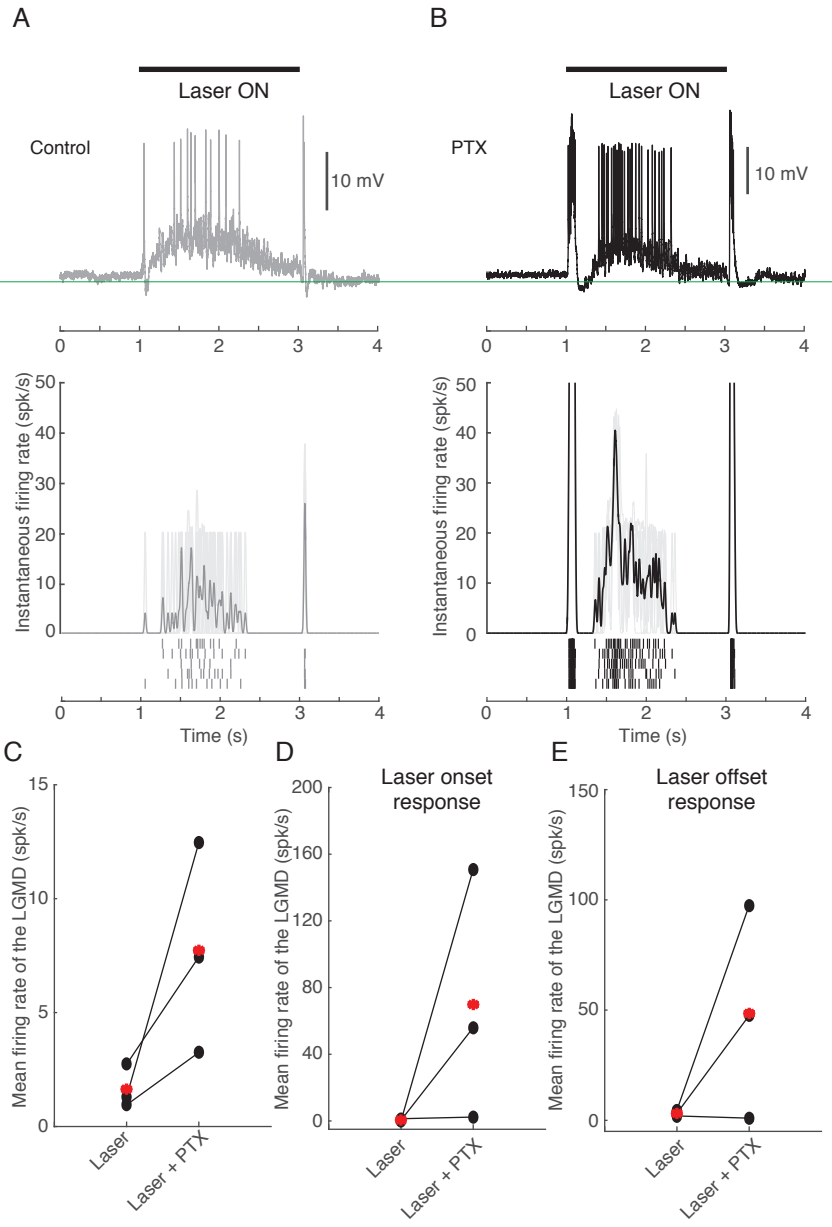

Wang et al., Fig. 3

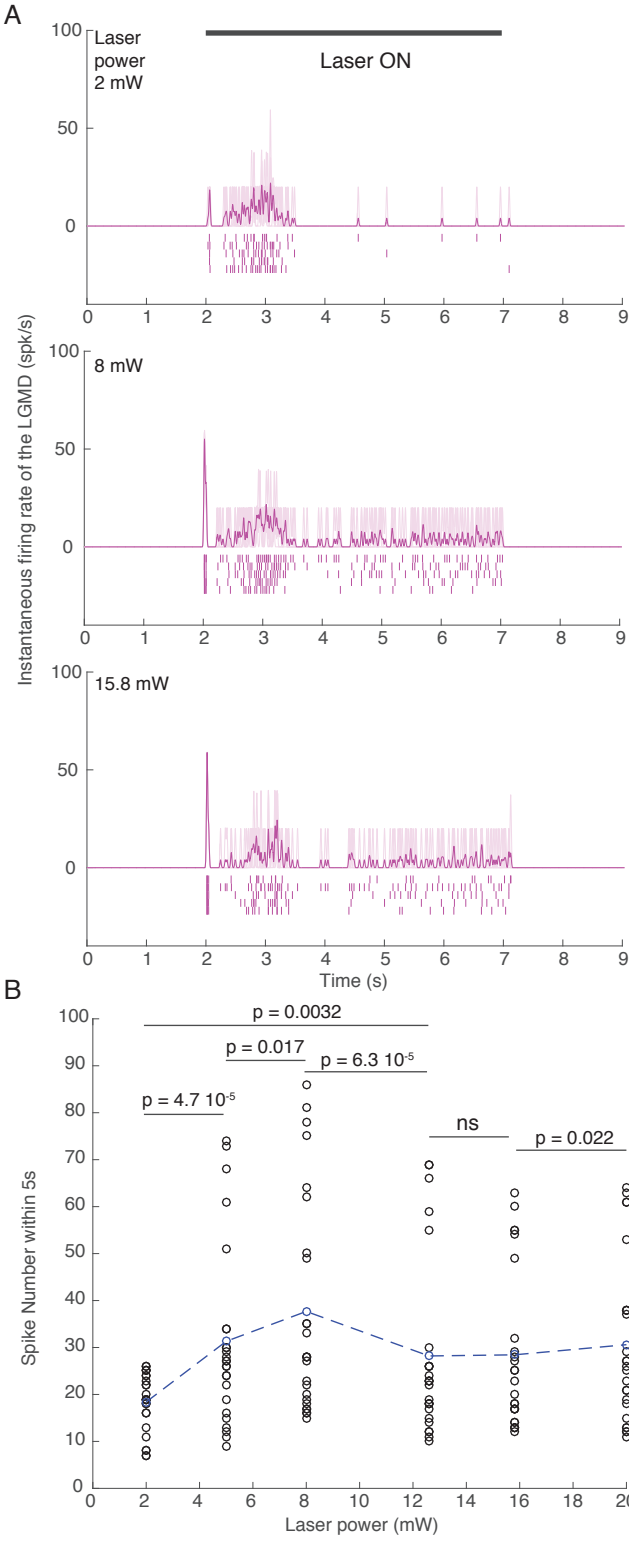

Wang et al., Fig. 4

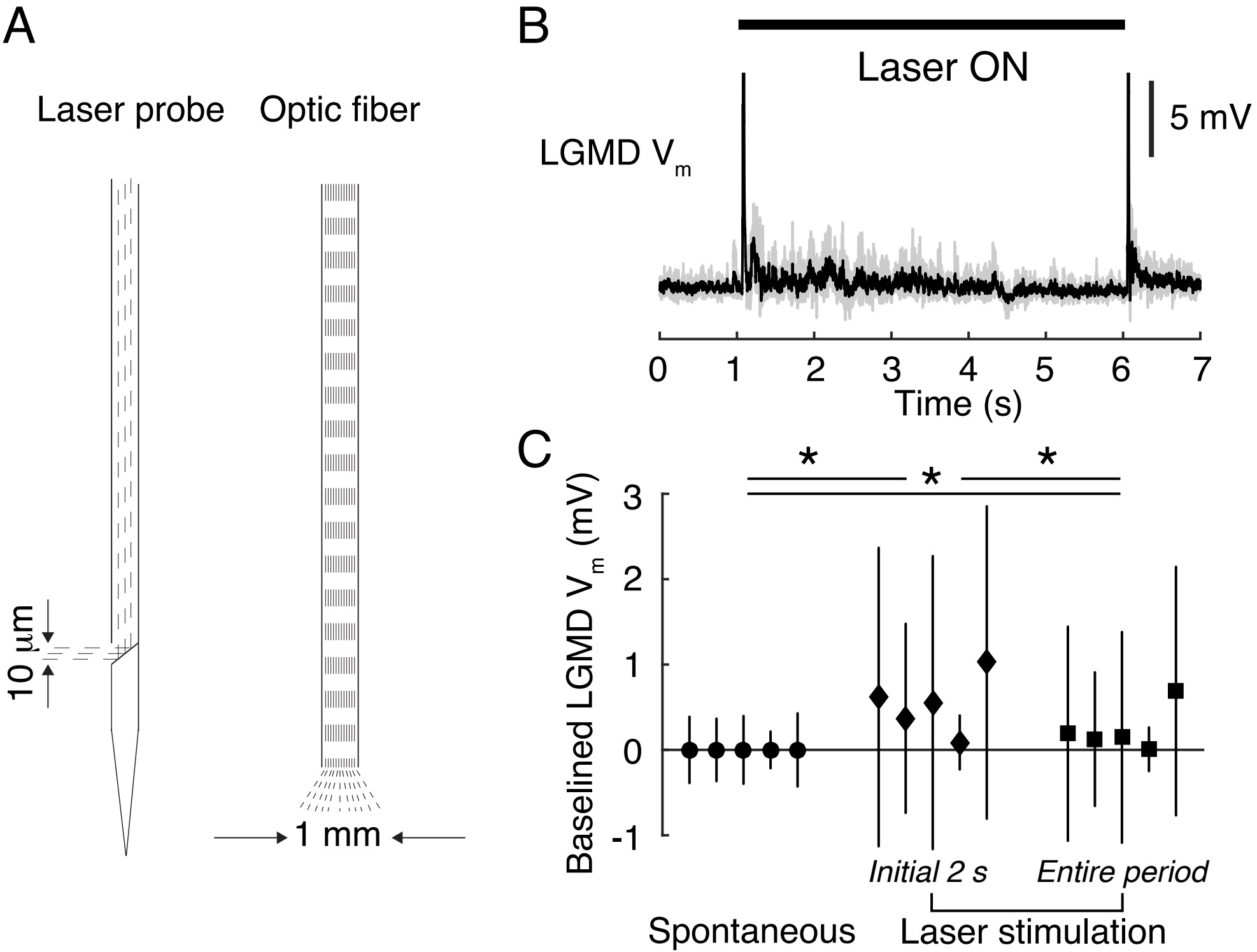

Wang et al., Fig. 5